PROCEEDINGS OF SCIENCE

Dark matter phenomenology in Z'2 broken singlet extended 2HDM

Julia Anabell Ziegler,[a,*] **Juhi Dutta,**[b] **Jayita Lahiri,**[a] **Cheng Li,**[c,d] **Gudrid Moortgat-Pick**[a,c] **and Sheikh Farah Tabira**[a]

[a] *II. Institut für Theoretische Physik, Universität Hamburg, Luruper Chaussee 149, 22761 Hamburg, Germany*

[b] *Homer L. Dodge Department of Physics and Astronomy, University of Oklahoma, Norman, OK 73019, USA*

[c] *Deutsches Elektronen-Synchrotron DESY, Notkestr. 85, 22607 Hamburg, Germany*

[d] *School of Science, Sun Yat-Sen University, Gongchang Road 66, 518107 Shenzhen, China*

E-mail: julia.ziegler@desy.de, juhi.dutta@ou.edu, jayita.lahiri@desy.de, gudrid.moortgat-pick@desy.de, cheng.li@desy.de, sheikh.farah.tabira@desy.de

Many different approaches have been made to explain the nature of dark matter (DM), but it remains and unsolved mystery of our universe. In this work we examine a type II two-Higgs-doublet model extended by a complex singlet (2HDMS), where the pseudo-scalar component of the singlet acts as a natural DM candidate. The DM candidate is stabilized by a Z_2' symmetry, which is broken spontaneously by the singlet acquiring a vacuum expectation value (vev). This vev in turn causes the scalar component of the singlet to mix with the scalar components of the two doublets, which results in three scalar Higgs particles. Additionally we aim to include an excess around 95 GeV, which was observed at CSM and LEP and can be explained by one of the three scalar Higgs particles.

After introducing the model, we apply experimental and theoretical constraints and find a viable benchmark point. We then look into the DM phenomenology as well as collider phenomenology.

DESY-23-167

The European Physical Society Conference on High Energy Physics (EPS-HEP2023)
21-25 August 2023
Hamburg, Germany

*Speaker

PoS(EPS-HEP2023)111

1. Introduction

Even though the Standard Model (SM) of particle physics has shown huge success in providing experimental predictions, there are many phenomena it can not explain, such as dark matter (DM), the matter-antimatter asymmetry, neutrino masses and other problems. This has led to many theories beyond the SM (BSM).

One natural choice for BSM models is the two-Higgs-doublet model (2HDM), which instead of one Higgs doublet, as in the SM, contains two Higgs doublets, leading to a richer phenomenology. A good overview can be found in ref. [1]. This model can be further extended with a complex singlet, leading to a still richer particle content in the Higgs sector and a natural DM candidate. This model was studied in ref. [2].

The aim of this work is to not only explain DM but also an excess around 95 GeV observed at the Compact Muon Solenoid (CMS) [3] and at the Large Electron–Positron Collider (LEP) [4]. Therefore we consider a 2HDMS, where the pseudo-scalar component of the singlet acts as a natural DM candidate, since it is massive, electrically neutral, colorless and stable. The stabilization of the DM is achieved through a Z_2' symmetry, which is spontaneously broken by the vacuum expectation value (vev) of the singlet. This vev leads to a mixing of the scalar sector. The total particle content of the Higgs sector results in three scalar, two pseudo-scalar, and two charged Higgs particles. Of the three scalars, the lightest one is chosen to have a mass of 95 GeV in accordance with the excess explained above, the second lightest is chosen to be SM-like with a mass of 125 GeV and the heavy one is chosen to have a mass of 900 GeV.

The possibility to accommodate the excess around 95 GeV in a 2HDMS was investigated in ref. [5]. The DM phenomenology in a 2HDMS without the singlet obtaining a vev was investigated in ref. [6].

This work wraps up the study done in ref. [7]. We first introduce the model and the considered constraints. Then we look into the DM phenomenology, namely relic density, indirect detection and direct detection of DM. Finally we look into the collider phenomenology at future electron and muon colliders and at the High Luminosity Large Hadron Collider (HL-LHC). We then conclude our work.

2. The 2HDMS model

As mentioned above, we consider a type II 2HDMS, where the singlet acquires a vev. The 2HDM part of the potential is symmetric under a $U(1)$ symmetry, to avoid charge-parity (CP) violation, and under a Z_2 symmetry, to avoid flavor-changing neutral currents (FCNC). The singlet part of the potential is symmetric under a Z_2' symmetry, to stabilize the DM candidate. The full Higgs sector potential is the sum of the 2HDM and the singlet potential and can be written as

$$V = V_{2HDM} + V_S \tag{1a}$$

$$\begin{aligned} V_{2HDM} = {} & m_{11}^2 \Phi_1^\dagger \Phi_1 + m_{22}^2 \Phi_2^\dagger \Phi_2 - [m_{12}^2 \Phi_1^\dagger \Phi_2 + h.c.] + \frac{\lambda_1}{2} (\Phi_1^\dagger \Phi_1)^2 \\ & + \frac{\lambda_2}{2} (\Phi_2^\dagger \Phi_2)^2 + \lambda_3 (\Phi_1^\dagger \Phi_1)(\Phi_2^\dagger \Phi_2) + \lambda_4 (\Phi_1^\dagger \Phi_2)(\Phi_2^\dagger \Phi_1) \end{aligned}$$

$$+\left[\frac{\lambda_5}{2}(\Phi_1^\dagger\Phi_2)^2+h.c.\right] \tag{1b}$$

$$V_S = m_S^2 S^\dagger S + \left[\frac{m_S'^2}{2}S^2+h.c.\right] + \left[\frac{\lambda_1''}{24}S^4+h.c.\right]+\left[\frac{\lambda_2''}{6}(S^2S^\dagger S)+h.c.\right]+\frac{\lambda_3''}{4}(S^\dagger S)^2 + S^\dagger S[\lambda_1'\Phi_1^\dagger\Phi_1+\lambda_2'\Phi_2^\dagger\Phi_2]+[S^2(\lambda_4'\Phi_1^\dagger\Phi_1+\lambda_5'\Phi_2^\dagger\Phi_2)+h.c.], \tag{1c}$$

where $h.c.$ stands for the hermitian conjugate, $\Phi_{1,2}$ denote the two doublets and S denotes the singlet. For simplicity we set the parameters $\lambda_1'' = \lambda_2''$.

After spontaneous symmetry breaking both doublets and the singlet obtain vevs. They can be expanded around the vevs and written in terms of real and imaginary component. Where the real components give rise to the scalar particles and the imaginary components give rise to the pseudo-scalar particles. The charged particles results from the upper components of the doublets and do no acquire a vev. The doublet and singlet fields can then be written as

$$\Phi_i = \begin{pmatrix} \phi_i^+ \\ \frac{1}{\sqrt{2}}(v_i+\rho_i+i\eta_i)\end{pmatrix} \qquad \langle\Phi_i\rangle = \begin{pmatrix}0\\ \frac{v_i}{\sqrt{2}}\end{pmatrix}, \quad i=1,2 \tag{2a}$$

$$S = \frac{1}{\sqrt{2}}(v_S+\rho_S+iA_S) \qquad \langle S\rangle = \frac{v_S}{\sqrt{2}}, \tag{2b}$$

where $v_{1,2}$ denote the vevs of the two doublets and v_S the singlet vev. The imaginary component of the singlet A_S is the DM candidate.

After diagonalization of the mass matrix we are left with three scalars h_1, h_2, h_3, two pseudo-scalars A, A_S, and two charged Higgs particles $H^\pm$, as well as two charged Goldstone bosons $G^\pm$ and a pseudo-scalar Goldstone boson G^0. The mixing of these mass eigenstates is as follows, further details can be found in ref. [7]:

$$\begin{pmatrix}h_1\\h_2\\h_3\end{pmatrix} = R\begin{pmatrix}\rho_1\\\rho_2\\\rho_S\end{pmatrix}, \quad \begin{pmatrix}A\\G^0\end{pmatrix} = R^A\begin{pmatrix}\eta_1\\\eta_2\end{pmatrix}, \quad \begin{pmatrix}A_S\end{pmatrix} = \begin{pmatrix}A_S\end{pmatrix}, \quad \begin{pmatrix}H^\pm\\G^\pm\end{pmatrix} = R^\pm\begin{pmatrix}\phi_1^+\\\phi_2^+\end{pmatrix}, \tag{3}$$

where R is the scalar, R^A the pseudo-scalar and $R^\pm$ the charged mixing matrix and A_S does not mix with the other mass eigenstates.

In a type II 2HDMS the up-type quarks couple to the second doublet Φ_2 and the down-type quarks and leptons couple to the first doublet Φ_1 to obtain their masses. The singlet has no direct coupling to the SM particles. Hence the pseudo-scalar DM candidate can couple to these only via the exchange of one of the scalars h_1, h_2, h_3.

2.1 Benchmark point

The free parameters in the interaction basis are:

$$\lambda_1,\lambda_2,\lambda_3,\lambda_4,\lambda_5,m_{12}^2,\tan\beta,v_S,m_S'^2,\lambda_1',\lambda_2',\lambda_4',\lambda_5',\lambda_1''=\lambda_2'',\lambda_3''. \tag{4}$$

After a basis change these parameters can be expressed via the mass basis parameters:

$$m_{h_1}, m_{h_2}, m_{h_3}, m_A, m_{A_S}, m_{H^\pm}, \delta'_{14} = \lambda'_4 - \lambda'_1, \delta'_{25} = \lambda'_5 - \lambda'_2,$$
$$\tan\beta, v_S, c_{h_1bb}, c_{h_1tt}, \tilde{\mu}^2, m'^2_S, alignm, \tag{5}$$

where m_X denotes the mass eigenvalue of the mass eigenstates $X = h_1, h_2, h_3, A, A_S, H^\pm$, the parameters $\delta'_{14} = \lambda'_4 - \lambda'_1$ and $\delta'_{25} = \lambda'_5 - \lambda'_2$, the reduced couplings $c_{h_1dd} = \frac{R_{11}}{\cos\beta}$ and $c_{h_1uu} = \frac{R_{12}}{\sin\beta}$, $\tilde{\mu}^2 = \frac{m_{12}^2}{\sin\beta\cos\beta}$, with $\tan(\beta) = \frac{v_2}{v_1}$, and the parameter assuring alignment limit $alignm = |\sin(\beta - \alpha_1 - \alpha_3 \cdot \mathrm{sgn}(\alpha_2))| \approx 1$, with $\alpha_{1,2,3}$ being the angles of the scalar rotation matrix R. The motivation to choose these parameters as input parameters, as well as the full basis change equations can be found in ref. [7].

Our analysis starts from the benchmark point BP1. The corresponding values of the mass basis parameters can be found in table 1. This benchmark point was checked against theoretical

m_{h_1}	m_{h_2}	m_{h_3}	m_A	m_{A_S}
95 GeV	125.09 GeV	900 GeV	900 GeV	325.86 GeV
$m_{H^\pm}$	m'^2_S	δ'_{14}	δ'_{25}	$\tan(\beta)$
900 GeV	-4.809×10^4 GeV^2	−9.6958	0.2475	10
v_S	c_{h_1bb}	c_{h_1tt}	$alignm$	$\tilde{\mu}^2$
239.86 GeV	0.2096	0.4192	0.9998	8.128×10^5 GeV^2

Table 1: Benchmark point BP1 in the mass basis

constraints, such as bounded from below (bfb), unitarity (checked with `SPheno-v4.0.5` [8]) and vacuum stability constraints (checked with `EVADE` [9, 10]), as well as experimental constraints, such as constraints on the Higgs sector (checked with `HiggsTools` [11–16]), on the DM relic density (upper bounds from `Planck` [17]), on the DM indirect detection cross section (upper bounds from `Fermi-LAT` [18, 19]) and on the DM direct detection cross section (upper bounds from `LUX-ZEPLIN` [20]). Furthermore the lightest scalar h_1 was chosen to have a mass of 95 GeV, in accordance with the excess at CMS and LEP, mentioned in the introduction. The second lightest scalar h_2 was chosen to be the SM-like Higgs with a mass of around 125 GeV.

The programs used to produce the following results are `SARAH-v4.14.3` [21] for the implementation of the model, `SPheno-v4.0.5` [8] for the generation of the spectrum, which in turn is used as input for `micrOmegas-v5.2.13` [22], which is used for the DM phenomenology. For the collider phenomenology we use `MG5_aMC_v3.4.1` [23, 24], `Pythia_v8` [25], `Delphes-v3.5.0` [26], `MadAnalysis-v5` [27] and `WHIZARD` [28].

3. Results

3.1 Dark matter phenomenology

In this section we look into the change of DM observables, namely relic density, indirect detection cross section and direct detection cross section, under variation of the DM mass m_{A_S} and the parameters m'^2_S around the benchmark point BP1. The results can be seen in figure 1. The hatched areas show which regions are excluded by the theoretical and experimental constraints.

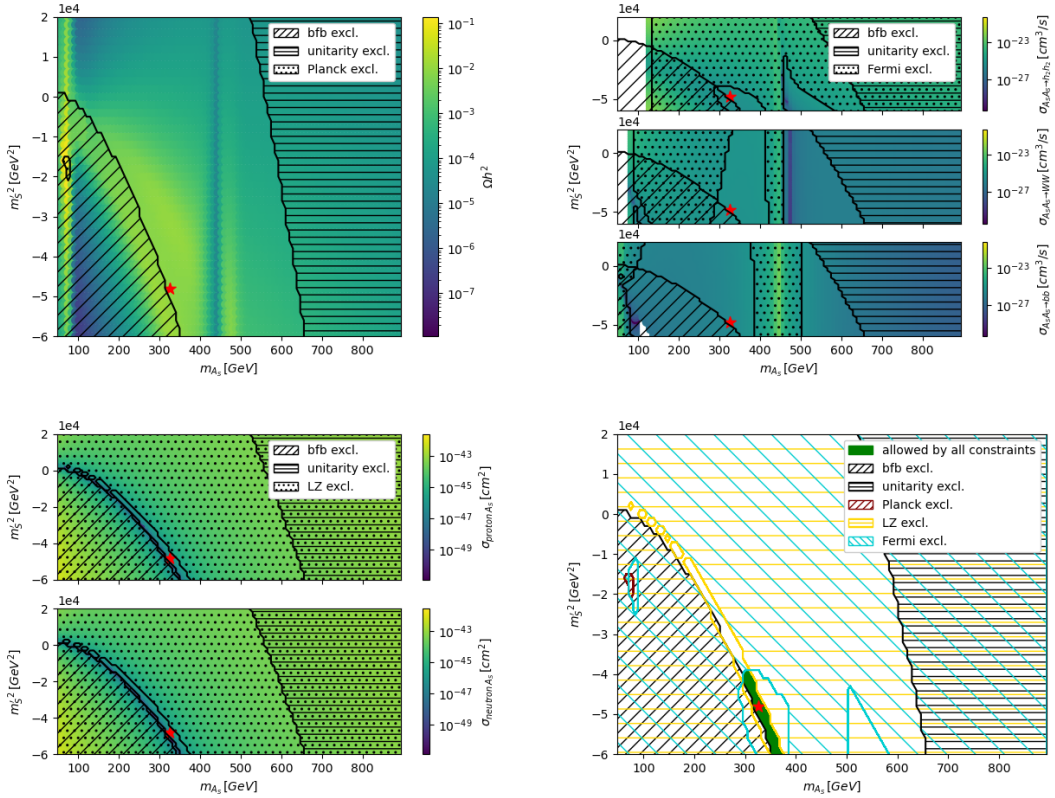

Figure 1: DM observables for varying the DM mass m_{A_S} and $m_S'^2$ around BP1 (marked with a red star). The color coding shows the relic density Ωh^2 (top left), indirect detection cross section $\sigma_{A_SA_S\to h_2h_2/WW/bb}$ (top right), direct detection cross section $\sigma_{\text{proton/neutron}A_S}$ (bottom left) and the allowed parameter regions under combination of all constraints (bottom right).

The bfb, unitarity and vacuum stability constraints, as well as bounds on the Higgs sector apply to all three DM observables. Only those constraints which actually constrain the scanned parameter space are shown in the plots. In addition for the relic density (top left) constraints from `Planck`, for the indirect detection cross section (top right) constraints from `Fermi-LAT` and for the direct detection cross section (bottom left) constraints from `LUX-ZEPLIN` (`LZ`) are shown as dotted areas. In the plot on the bottom right, all these constraints are combined to show the allowed parameter space. As can be seen, under all constraints only a small strip around BP1 is allowed. The strongest constraints, on the parameter space shown here, come from `Fermi-LAT` and `LZ`.

The behaviour of the relic density shows some interesting features. For example a dip around $m_{A_S} \approx 62.5\,\text{GeV} \approx \frac{m_{h_2}}{2}$, where resonant annihilation of two A_S into one h_2 is possible. Between this peak and $m_{A_S} \approx 95\,\text{GeV} \approx m_{h_1}$ the relic density is quite high, then it drops again as the annihilation channel of two A_S into two h_1 opens up and keeps the relic density at a low level, however increasing slowly for higher values of m_{A_S}. At $m_{A_S} \approx 450\,\text{GeV} \approx \frac{m_{h_3}}{2}$ another dip appears, as resonant annihilation of two A_S into one h_3 decreases the relic density.

For the indirect detection cross section the three main annihilation channels $A_SA_S \to h_2h_2/WW/bb$ (from top to bottom) are shown. Some regions are white as the cross section is too low and

no values are returned. The dip in the the relic density plot around $m_{A_S} \approx 450\,\text{GeV} \approx \frac{m_{h_3}}{2}$ shows up as a peak in the indirect detection plot, as both observables behave roughly inversely. (When more DM annihilates, the indirect detection cross section, which is just the annihilation cross section, grows. This also means that after annihilation less DM is left in the universe, hence relic density is decreased.)

The direct detection cross section is shown for scattering of a DM particle on a proton and on a neutron. Both plots look very similar and show that BP1 lies right in a minimum of the cross section.

3.2 Collider phenomenology

3.2.1 Future lepton colliders

In this section we look into the production cross sections of different final states including DM particles at the proposed future electron and at muon colliders under variation of the center of mass energy $\sqrt{s}$, for BP1. At these kind of colliders the heavy scalar h_3 could be produced directly from lepton and anti-lepton and then decay into two DM particles A_S. Possible final states include either only $A_S A_S$ or additional Z bosons or photons γ. The results can be seen in figure 2.

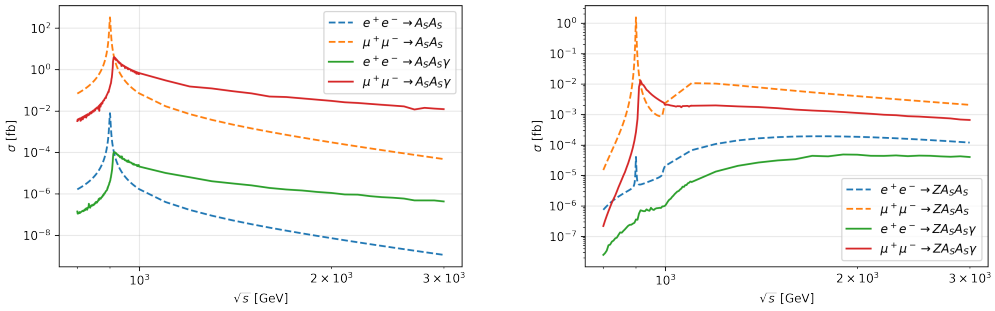

Figure 2: Production cross section for varying center of mass energy $\sqrt{s}$ at electron (blue and green lines) and muon (orange and red lines) collider. Shown are the results for production of two DM particles A_S (left) without (dotted lines) and with (solid lines) a photon γ in the final state and the same with an additional Z boson in the final state (right).

On the left the processes $e^+e^-/\mu^+\mu^- \to A_S A_S$ are shown without and with a photon in the final state (initial state radiation) are shown. Since the DM particles cannot be detected, only the photon and missing energy would be measured.

On the right the processes $e^+e^-/\mu^+\mu^- \to Z A_S A_S$ are shown again without and with a photon in the final state. In this case the Z boson and the photon and missing energy would be detected.

In both plots a peak around $\sqrt{s} \approx 900\,\text{GeV} \approx m_{h_3}$ can be seen, as resonant production of one h_3 is possible, which would then decay into two A_S in the final state. Furthermore in both plots the cross sections for the muon collider are higher than for the electron collider, which one would expect since the muon has stronger Yukawa couplings to the Higgs doublets.

For all processes with photons in the final state the following cut on the photon energy was employed: $E_\gamma > 10\,\text{GeV}$ and for the photon angle: $\theta > 7°$ in order to avoid divergences [29].

3.2.2 HL-LHC

For the analysis at HL-LHC, the main production channels for the heavy scalar h_3 are gluon gluon fusion (GGF) and vector boson fusion (VBF). The h_3 could then decay into two DM particles A_S. For both processes the significance $\mathcal{S} = \sqrt{2 \times \left[(s+b)\ln(1+\frac{s}{b}) - s\right]}$ of the signal s over the total SM background b is calculated while taking into account some cuts which can be found in ref. [7]. The results are for BP1 are:

$$\text{GGF: } \mathcal{S} = 1.356\,\sigma$$
$$\text{VBF: } \mathcal{S} = 0.007\,\sigma,$$

which is very low. However in another benchmark or by using machine learning techniques these results could be improved.

4. Conclusions

In this work we have investigated the DM phenomenology in a 2HDMS, where the DM candidate is the pseudo-scalar component of the singlet. We have found a benchmark point which is allowed under theoretical and experimental constraints and which also accommodates an excess found at CMS and LEP, which can be interpreted as a scalar Higgs particle with a mass of 95 GeV.

Furthermore we have looked into the production prospects at future lepton colliders and found potentially promising results. These could be further improved when taking beam polarization into account, as well as doing broader parameter scans and looking into more benchmarks. Future studies on this are in progress. The significance at HL-LHC however is rather low in the studied benchmark. Comprehensive parameter scans are planned for the future.

This work is a short summary of the study done in ref. [7]. Further information and explanations can be found there.

Acknowledgements

JZ, JD, JL and GMP acknowledge support by the Deutsche Forschungsgemeinschaft (DFG, German Research Foundation) under Germany's Excellence Strategy EXC 2121 "Quantum Universe"- 390833306. JD acknowledges support from the HEP Dodge Family Endowment Fellowship at the Homer L.Dodge Department of Physics & Astronomy at the University of Oklahoma.

References

[1] G. Branco, P. Ferreira, L. Lavoura, M. Rebelo, M. Sher, and J. P. Silva, *Theory and phenomenology of two-higgs-doublet models*, *Physics Reports* **516** (Jul, 2012) 1–102, [arXiv:1106.0034].

[2] S. Baum and N. R. Shah, *Two higgs doublets and a complex singlet: disentangling the decay topologies and associated phenomenology*, *Journal of High Energy Physics* **2018** (dec, 2018) [arXiv:1808.02667].

[3] A. M. Sirunyan et al., *Search for a standard model-like higgs boson in the mass range between 70 and 110 GeV in the diphoton final state in proton-proton collisions at* $\sqrt{s} = 8$ *and* 13 *TeV*, *Physics Letters B* **793** (jun, 2019) 320–347, [arXiv:1811.08459].

[4] G. Abbiendi et al., *Search for the standard model higgs boson at LEP*, *Physics Letters B* **565** (jul, 2003) 61–75, [hep-ex/0306033].

[5] S. Heinemeyer, C. Li, F. Lika, G. Moortgat-Pick, and S. Paasch, *A 96 gev higgs boson in the 2hdm plus singlet*, arXiv:2112.11958.

[6] J. Dutta, G. Moortgat-Pick, and M. Schreiber, *Phenomenology of the dark matter sector in the 2hdm extended with complex scalar singlet*, arXiv:2203.05509.

[7] J. Dutta, J. Lahiri, C. Li, G. Moortgat-Pick, S. F. Tabira, and J. A. Ziegler, *Dark matter phenomenology in 2hdms in light of the 95 gev excess*, arXiv:2308.05653.

[8] W. Porod, *SPheno, a program for calculating supersymmetric spectra, SUSY particle decays and SUSY particle production at e+ e− colliders*, *Computer Physics Communications* **153** (jun, 2003) 275–315, [hep-ph/0301101v4].

[9] W. G. Hollik, G. Weiglein, and J. Wittbrodt, *Impact of Vacuum Stability Constraints on the Phenomenology of Supersymmetric Models*, *JHEP* **03** (2019) 109, [arXiv:1812.04644].

[10] P. M. Ferreira, M. Mühlleitner, R. Santos, G. Weiglein, and J. Wittbrodt, *Vacuum Instabilities in the N2HDM*, *JHEP* **09** (2019) 006, [arXiv:1905.10234].

[11] H. Bahl, T. Biekötter, S. Heinemeyer, C. Li, S. Paasch, G. Weiglein, and J. Wittbrodt, *HiggsTools: BSM scalar phenomenology with new versions of HiggsBounds and HiggsSignals*, *Comput. Phys. Commun.* **291** (2023) 108803, [arXiv:2210.09332].

[12] P. Bechtle, O. Brein, S. Heinemeyer, G. Weiglein, and K. Williams, *HiggsBounds: Confronting arbitrary higgs sectors with exclusion bounds from LEP and the tevatron*, *Computer Physics Communications* **181** (jan, 2010) 138–167, [arXiv:0811.4169].

[13] P. Bechtle, O. Brein, S. Heinemeyer, O. Stål, T. Stefaniak, G. Weiglein, and K. E. Williams, HiggsBounds – 4*: Improved Tests of Extended Higgs Sectors against Exclusion Bounds from LEP, the Tevatron and the LHC*, *Eur. Phys. J. C* **74** (2014), no. 3 2693, [arXiv:1311.0055].

[14] P. Bechtle, D. Dercks, S. Heinemeyer, T. Klingl, T. Stefaniak, G. Weiglein, and J. Wittbrodt, *HiggsBounds-5: Testing Higgs Sectors in the LHC 13 TeV Era*, *Eur. Phys. J. C* **80** (2020), no. 12 1211, [arXiv:2006.06007].

[15] P. Bechtle, S. Heinemeyer, O. Stål, T. Stefaniak, and G. Weiglein, *HiggsSignals: Confronting arbitrary Higgs sectors with measurements at the Tevatron and the LHC*, *Eur. Phys. J. C* **74** (2014), no. 2 2711, [arXiv:1305.1933].

[16] P. Bechtle, S. Heinemeyer, T. Klingl, T. Stefaniak, G. Weiglein, and J. Wittbrodt, *HiggsSignals-2: Probing new physics with precision Higgs measurements in the LHC 13 TeV era*, *Eur. Phys. J. C* **81** (2021), no. 2 145, [arXiv:2012.09197].

[17] **Planck** Collaboration, N. Aghanim et al., *Planck 2018 results. VI. Cosmological parameters*, *Astron. Astrophys.* **641** (2020) A6, [arXiv:1807.06209].

[18] **Fermi-LAT** Collaboration, M. Ackermann et al., *Constraining Dark Matter Models from a Combined Analysis of Milky Way Satellites with the Fermi Large Area Telescope*, *Phys. Rev. Lett.* **107** (2011) 241302, [arXiv:1108.3546].

[19] **Fermi-LAT, DES** Collaboration, A. Albert et al., *Searching for Dark Matter Annihilation in Recently Discovered Milky Way Satellites with Fermi-LAT*, *Astrophys. J.* **834** (2017), no. 2 110, [arXiv:1611.03184].

[20] J. Aalbers et al., *First dark matter search results from the LUX-ZEPLIN (LZ) experiment*, *Physical Review Letters* **131** (jul, 2023) [arXiv:2207.03764].

[21] F. Staub, *SARAH 4 : A tool for (not only SUSY) model builders*, *Comput. Phys. Commun.* **185** (2014) 1773–1790, [arXiv:1309.7223].

[22] G. Bélanger, F. Boudjema, A. Goudelis, A. Pukhov, and B. Zaldívar, *micrOMEGAs5.0 : Freeze-in*, *Computer Physics Communications* **231** (oct, 2018) 173–186, [arXiv:1801.03509].

[23] J. Alwall, R. Frederix, S. Frixione, V. Hirschi, F. Maltoni, O. Mattelaer, H. S. Shao, T. Stelzer, P. Torrielli, and M. Zaro, *The automated computation of tree-level and next-to-leading order differential cross sections, and their matching to parton shower simulations*, *JHEP* **07** (2014) 079, [arXiv:1405.0301].

[24] J. Alwall, M. Herquet, F. Maltoni, O. Mattelaer, and T. Stelzer, *MadGraph 5 : Going Beyond*, *JHEP* **06** (2011) 128, [arXiv:1106.0522].

[25] C. Bierlich, S. Chakraborty, N. Desai, L. Gellersen, I. Helenius, P. Ilten, L. Lönnblad, S. Mrenna, S. Prestel, C. T. Preuss, T. Sjöstrand, P. Skands, M. Utheim, and R. Verheyen, *A comprehensive guide to the physics and usage of pythia 8.3*, arXiv:2203.11601.

[26] J. de Favereau, C. Delaere, P. Demin, A. Giammanco, V. Lemaître, A. Mertens, and M. Selvaggi, *DELPHES 3: a modular framework for fast simulation of a generic collider experiment*, *Journal of High Energy Physics* **2014** (feb, 2014) [arXiv:1307.6346].

[27] E. Conte, B. Fuks, and G. Serret, *MadAnalysis 5, A User-Friendly Framework for Collider Phenomenology*, *Comput. Phys. Commun.* **184** (2013) 222–256, [arXiv:1206.1599].

[28] W. Kilian, T. Ohl, and J. Reuter, *WHIZARD: Simulating Multi-Particle Processes at LHC and ILC*, *Eur. Phys. J. C* **71** (2011) 1742, [arXiv:0708.4233].

[29] J. Kalinowski, W. Kotlarski, P. Sopicki, and A. F. Zarnecki, *Simulating hard photon production with WHIZARD*, *Eur. Phys. J. C* **80** (2020), no. 7 634, [arXiv:2004.14486].

PoS(EPS-HEP2023)111